The rapid resetting of the Ca isotopic signatures of calcite at ambient temperature during its congruent dissolution, precipitation, and at equilibrium

Eric H Oelkers, Philip a E Pogge von Strandmann, Vasileios Mavromatis, Philip A.E. Pogge von Strandmann

The rapid resetting of the Ca isotopic signatures of calcite at ambient temperature during its congruent dissolution, precipitation, and at equilibrium

Eric H. Oelkers [1,2,*] Philip A.E. Pogge von Strandmann[2,3], and Vasileios Mavromatis[1,4]

[1]Géosciences Environnement Toulouse (GET), CNRS, UMR5563, 14 Avenue Edouard Belin, 31400 Toulouse, France

[2]Earth Sciences, University College London, Gower Street, London WC1E 6BT, United Kingdom

[3] Department of Earth and Planetary Sciences Birkbeck, University of London, Gower Street, London WC1E 6DT, United Kingdom

[4]Institute of Applied Geosciences, Graz University of Technology, Rechbauerstrasse 12, 8010 Graz, Austria

Abstract- This study provides direct experimental evidence of the resetting of the calcium (Ca) isotope signatures of calcite in the presence of an aqueous fluid during its congruent dissolution, precipitation, and at equilibrium at ambient temperatures over week-long timescales. Batch reactor experiments were performed at 25 ºC in aqueous NaCl solutions; air or CO_2-gas mixtures were bubbled through this fluid to fix pH. During congruent calcite dissolution, the fluid became enriched in isotopically heavy Ca, and the Ca isotope composition continued to become heavier after the fluid attained bulk chemical equilibrium with the mineral; the $\delta^{44/42}$Ca composition of the fluid was up to 0.8 ‰ higher than the dissolving calcite at the end of the dissolution experiments. Calcite precipitation was provoked by increasing the reactor fluid pH after chemical equilibrium had been attained via dissolution. Rayleigh isotope fractionation effects were observed immediately after the pH was increased and rapid calcite precipitation occurred. However, isotopic exchange continued after the system chemically equilibrated, eradicating this Rayleigh signal. Taken together, these observations 1) confirm dynamic mineral-fluid equilibrium (i.e. dissolution and precipitation occur at equal, non-zero rates at equilibrium), and 2) indicate that isotopic compositions of calcite can readily equilibrate even when this mineral is in bulk chemical equilibrium with its coexisting fluid. This latter observation suggests the preservation of paleo-environmental isotopic signatures in calcite may require a combination of the isolation

[*] Corresponding Author: e-mail: e.oelkers@ucl.ac.uk; Telephone +44 (0)20 7673 5632

of fluid-mineral system from external chemical input and/or the existence of a yet to be defined calcite dissolution/precipitation inhibition mechanism.

1. INTRODUCTION

The Ca isotope compositions of natural calcium carbonates are widely used to illuminate a large number of natural processes including the global Ca cycle (Zhu and Macdougall, 1998; Heuser *et al.,* 2005; Tipper *et al.,* 2006; Fantle and Tipper, 2014; Sawaki *et al.,* 2014; Farkas et al., 2016; Silva-Tamayo *et al.,* 2018), continental weathering rates (Tipper *et al.,* 2008; Blattler *et al.,* 2011; Hindshaw *et al.,* 2011; 2013; Kasemann *et al.,* 2014), soil formation (Page *et al.,* 2008; Cenki-Tok *et al.,* 2009; Holmden and Belanger; 2010), past and present environmental conditions (Kasemann *et al.,* 2005; Owen *et al.,* 2016), and the mechanism of biomineral formation (Pruss e*t al.,* 2018). Moreover, the Ca isotope signatures of natural waters are being used to trace their origin (Druhan *et al.,* 2013; Yan *et al.,* 2016; Lyons *et al.,* 2017; Li *et al.,* 2018). These potential applications have motivated an increasing number of studies focused on the measurement and behavior of calcium isotopic compositions in low-temperature systems (e.g. DePaolo, 2004; Tang e*t al.,* 2008, 2012; Fantle and Tipper, 2014; AlKhatib and Eisenhauer, 2017; Wang *et al.,* 2017). A substantial number of experimental studies have concluded that isotopically light Ca is preferentially incorporated into calcium carbonate minerals (Lemarchand *et al.,* 2004; Marriott *et al.,* 2004; Gussone *et al.,* 2005, 2011; Reynard *et al.,* 2011; Tang *et al.,* 2008, 2012).

The interpretation of stable isotope compositions of natural minerals and waters commonly relies on two assumptions. The first is that once a mineral is precipitated it retains its original isotopic signal and thus preserves information about its formation conditions. This assumption serves as the basis for paleo-environmental and paleo temperature

55 reconstructions (e.g. Marshall, 1992; Koch, 1998; Nagler *et al.,* 2000; Leng and Marshall,
56 2004; Fairchild et al., 2006). The second assumption is that stable isotope signatures are
57 transferred conservatively to the fluid phase during congruent mineral dissolution[1] (e.g.
58 Jacobson and Holmden, 2008; Ryu *et al.,* 2011; Turchyn and DePaolo, 2011). This latter
59 assumption has been adopted to trace flow paths and the origin of fluids in natural systems
60 (e.g. Grazis and Feng, 2004; Wiederhold, 2015).

61 A number of studies, however, have presented evidence that the isotopic compositions
62 of carbonate minerals can be altered while dissolving stoichiometrically or when the mineral
63 is in bulk chemical equilibrium with the fluid phase over the course of hours to days. For
64 example, Pearce e*t al.* (2012) observed that Mg isotopes fractionated substantially during
65 stoichiometric magnesite dissolution at 150 and 200 °C, and that the fluid Mg isotopic
66 composition continued to evolve after bulk equilibrium was attained between the mineral
67 and fluid. Mavromatis *et al.* (2016) reported that the Ba isotope signature of precipitated
68 witherite continued to evolve in closed system experiments after the attainment of bulk
69 mineral-aqueous fluid equilibrium. Mavromatis *et al*. (2017a) observed the continued Sr
70 isotope exchange in strontianite in closed system reactors after the attainment of bulk
71 mineral-aqueous fluid equilibrium in both dissolution and precipitation experiments. Similar
72 observations have been made for Mg isotope exchange in hydromagnesite (Oelkers *et al.,*
73 2018), Mg and Ca isotope exchange in dolomite (Perez-Fernandez *et al.,* 2017), Mg isotope
74 exchange in amorphous calcium carbonate (ACC) and Mg-rich calcite (Mavromatis et al.,
75 2017b), Ba isotope exchange in barite (Curti *et al.,* 2010), and Si isotope exchange in quartz
76 (Liu et al., 2016). Mavromatis *et al.* (2012) and Shirokova *et al.* (2013) observed the

[1] The term congruent dissolution in this study refers to stoichiometric dissolution without the formation of secondary minerals nor evidence for re-crystallisation.

continuous re-equilibration of Mg isotopes between the hydrous Mg carbonate minerals hydromagnesite/dypingite and its co-existing aqueous fluid at ambient temperatures during experiments that lasted no more than 4 weeks. In a follow-up study, Mavromatis *et al.* (2015) reported the continuous re-equilibration of C isotopes between the hydromagnesite/dypingite and its co-existing aqueous fluid at the same conditions. The resetting of mineral isotopic signatures in natural sedimentary rocks has been referred to as 'diagenetic effects'; a number of studies have concluded that these effects influence the calcium isotopic signatures of natural calcium carbonate minerals (Fantle and DePaolo, 2007; Teichert *et al.,* 2009; Fantle *et al.,* 2010; Druhan *et al.,* 2013; Fantle and Higgins, 2004; Harouaka et al., 2014; Jost *et al.,* 2014; Steefel *et al.,* 2014; Fantle, 2015; Chanda et al., 2019).

Isotope exchange towards mineral-fluid *isotopic equilibrium* during congruent dissolution and at *bulk chemical equilibrium* is consistent with the concept of dynamic equilibrium (van't Hoff, 1884). This concept is often invoked for the interpretation of mineral dissolution and precipitation rates (e.g. Aagaard and Helgeson, 1982; Oelkers *et al.,* 1994; Schott and Oelkers, 1995; Oelkers, 2001; Schott et al., 2009, 2012). Critical to the concept of dynamic equilibrium as applied to mineral-fluid interaction is that chemical reactions proceed by two-way mass transfer, the combination of forward dissolution and reverse precipitation. Note that the reverse precipitation is of the identical material that is removed from the mineral during forward dissolution. In undersaturated fluids, the rate of the forward dissolution is faster than that of the reverse precipitation and the net overall process is mineral dissolution, whereas in supersaturated solutions the rate of the reverse precipitation is faster than that of forward dissolution and the overall net reaction is mineral precipitation. At equilibrium, the rate of forward dissolution is equal to that of the reverse precipitation

such that there is no net bulk chemical transfer. As such, even if the original removal of an element from a mineral via forward dissolution is isotopically conservative[2], isotopic fractionation can occur as a consequence of the coupled reverse precipitation, both during bulk dissolution and at equilibrium (see Steefel et al., 2014). To assess the degree to which such processes can effect the isotopic compositions of calcite, this study followed the temporal evolution of calcium isotope compositions of the fluid phase during the congruent dissolution, precipitation, and at chemical equilibrium during ambient temperature closed-system calcite-water experiments. Results of shorter than month-long experiments demonstrate that 1) calcium isotopes are not conservatively transferred the fluid during congruent calcite dissolution, 2) the calcium isotopic composition of calcite and its co-existing fluid phase continue to evolve after the fluid has attained bulk chemical equilibrium, and 3) kinetically mediated isotopic signatures obtained during rapid calcite precipitation can be subsequently re-equilibrated by further fluid-calcite interaction. These observations require that a substantial portion of the calcium within the calcite is transferred in and out of the fluid phase in experiments performed at conditions at or near to calcite/aqueous fluid bulk chemical equilibrium over the course of only a few weeks. The purpose of this article is to report the results of this experimental study and use these to assess the potential for the preservation of the original calcium isotope compositions of calcite in natural systems.

2. COMPUTATIONAL, EXPERIMENTAL, AND ANALYTICAL METHODS

The standard state adopted in this study for thermodynamic calculations is that of unit activity for pure minerals and H_2O at any temperature and pressure. For aqueous

[2] The term isotopically conservative in this manuscript refers to the transfer of a metal to an aqueous solution without zero isotopic fractionation.

123 species other than H_2O, the standard state is unit activity of the species in a hypothetical 1
124 molal solution referenced to infinite dilution at any temperature and pressure. Calcite
125 dissolution can be described using:

126 $Calcite = Ca^{2+} + CO_3^{2-}$ (1)

127 Taking account of the standard state, the law of mass action for this reaction is given by:

128 $K_{calcite} = a_{Ca^{2+}} a_{CO_3^{2-}}$ (2)

129 where $K_{calcite}$ stands for the equilibrium constant of reaction (1), and a_i represents the
130 activity of the subscripted aqueous species. The saturation state of an aqueous fluid with
131 respect to calcite can be quantified using the saturation index (*SI*) defined by

132 $SI = log\left(\frac{IAP}{K_{calcote}}\right)$

133 where IAP signifies for the aqueous ion activity product for reaction (1). Note that *SI* is
134 negative when the fluid is undersaturated with respect to calcite, positive when
135 supersaturated, and zero at fluid-calcite equilibrium. All thermodynamic calculations in this
136 study were performed using the PHREEQC computer code, together with its minteq.v4
137 database (Parkhurst and Appelo, 1999). Note that consideration of the analytical
138 uncertainties described below and those associated with the equilibrium constants present
139 in the minteq.v4 database, uncertainties associated with the calcite *SI* values calculated in
140 this study are on the order of ±0.1 (c.f. Voigt et al., 2018).

141 Two calcite-aqueous fluid batch reactor experiments were performed in 1000 ml
142 polypropylene reactors that were placed in a thermostated bath operating at 25 ^{o}C. Batch
143 reactor systems were chosen for this study to allow the fluid-water system to attain close to
144 bulk chemical equilibrium conditions, such that the isotopic evolution of the calcite and its

145 coexisting fluid phase could be observed in the absence of net chemical transfer between
146 the mineral and the fluid. Each batch reactor was equipped with a floating stirring bar that
147 rotated at ~250rpm. Experiment A was initiated by placing 2.35 g of calcite seed crystals
148 together with 965.4 g of an aqueous 0.01 mol/kg NaCl solution into the reactor. Air was
149 bubbled continuously through the reactor to fix pH. After 25 hours, the air was replaced by
150 pure CO_2 gas, lowering the fluid pH to 6.2 and provoking calcite dissolution; this part of
151 experiment A is referred to as the 'dissolution leg'. After an additional 193 hours, the pure
152 CO_2 gas was replaced with a 1% CO_2/N_2 gas mixture, raising the pH to 7.5 and provoking
153 calcite precipitation; this part of experiment A will be referred to as the 'precipitation leg'.
154 Experiment B was initiated by placing 2.03 g of calcite crystals, together with 1001.1 g of a
155 0.008 mol/kg NaCl solution into a reactor. Pure CO_2 gas was bubbled in the reactor fluid,
156 leading to a fluid pH of 6.3 and provoking calcite dissolution. Fluid samples were collected
157 regularly from each reactor using a 0.45 μm cellulose nitrate syringe filter. Prior to sampling,
158 the stirring bar was stopped to allow the suspended calcite to settle, minimizing changes in
159 the mass of solid present in the reactor due to sampling; no evidence of calcite passing
160 through the filter syringes during the sampling was observed. Note also that prior to their
161 introduction in the reactors, all gasses were saturated with a 0.01 mol/kg NaCl solution in a
162 separate fluid cell to avoid fluid evaporation in the reactors.

163 The solids used in these experiments were pure synthetic Merck reagent grade
164 calcite. The calcite used in the two experiments was taken from different containers of
165 Merck calcite, so differed slightly in their initial Ca isotope compositions (see below). Pure
166 synthetic calcite was chosen for these experiments to avoid any potential artifacts (such as
167 non-congruent dissolution) arising from the presence of impurities in the solids. Note that,
168 for example, the presence of Mg in biogenic calcite can provoke the dissolution of the

original solid and the precipitation of a more stable Mg-free calcite during isotope exchange experiments (Chanda et al., 2019). The solids in our study were not cleaned prior to use to avoid altering the surfaces prior to the experiments. The synthetic calcite consisted of 4 to 15 µm rhombohedral shaped crystals as shown in Fig. 1. X-ray Diffraction (XRD) and Energy Dispersive X-ray Spectroscopic (EDS) analyses confirmed that these crystals were pure calcite. Potential isotopic heterogeneities in these solids were not investigated. The specific surface area of the original calcite, as determined by multi-point krypton adsorption according to the BET method (Brunauer *et al.,* 1938) using a Quantachrome Instruments Autosorb 1, was 0.25 ± 10% m^2/g.

Aqueous fluids were regularly sampled from the reactor and analyzed for total alkalinity, pH, and calcium concentration. The alkalinity of each fluid sample was obtained by HCl titration using an automatic Schott TitroLine alpha $TA10^{plus}$ titrator with an uncertainty of ±2% and a detection limit of 5×10^{-5} eq kg^{-1}. Fluid phase pH measurements were performed at 25 °C immediately after sampling using a standard glass electrode, previously calibrated with 4.01, 6.86, and 9.18 NIST pH buffers; the precision of these measurements is ±0.02 pH units. The Ca concentration of each sample was measured by flame Atomic Absorption Spectroscopy (AAS) with an analytical uncertainty of ~3% and a detection limit of $6x10^{-7}$ M. The estimated uncertainties in these analyses are based on repeat analyses of selected samples performed regularly during the analyses.

The calcium isotope compositions of the fluid samples, as well as the bulk solids before and after the experiments were determined. Calcium isotope compositions are reported as $\delta^{44/42}$Ca normalized to the NIST Ca standard SRM915a (Schmidt *et al.,* 2001) consistent with

$$\delta^{44/42}Ca = \{[(^{44}Ca/^{42}Ca)_{sample} - (^{44}Ca/^{42}Ca)_{standard})]/(^{44}Ca/^{42}Ca)_{standard}\} \times 1000 \ ,$$

where $(^{44}Ca/^{42}Ca)_{sample}$ refers to the indicated isotopic molar ratio of the subscripted phase. Calcium was purified for isotopic analysis by ion exchange chromatography. Prior to separation, fluid samples were evaporated to dryness in a Savillex beaker, redissolved in concentrated aqueous HNO_3, evaporated to dryness again and dissolved in aqueous 2M HCl ready for loading on columns. For the solid calcite samples, ~10 mg of the solid was dissolved in concentrated aqueous HCl before being evaporated to dryness, then dissolved in concentrated aqueous HNO_3, evaporated to dryness again then dissolved in aqueous 2M HCl. An aliquot of this fluid was subsequently loaded onto the ion exchange resin, with 20–30 µg of Ca processed for each sample. Purification chemistry was performed in the isotope laboratories in the Earth Science Department at Oxford University. The method was previously described (Chu *et al.,* 2006; Reynard *et al.,* 2010; Blattler *et al.,* 2011), but, briefly, samples were purified through a 2-step ion-exchange method to isolate Ca^{2+}, where the first column used AG50W X12 (200-400 mesh) cation exchange resin, and the second column a Sr spec resin, to separate the isobaric interferences from strontium. Total Ca yields were greater than 99%, as determined by Ca content analysis of splits collected before and after the main collection bracket. The total procedural blank for Ca isotope analysis is ~0.5–0.7 ng, which is insignificant compared to the mass of sample used. Purified fluids were diluted to a concentration of 10 µg/ml, and measured on a Nu Instruments multi-collector inductively coupled plasma mass spectrometer (MC-ICP-MS), using a sample-standard bracketing system relative to SRM-915a. With an uptake rate of 100 µl/min, and using a Nu Instruments DSN desolvating nebulizer, a sensitivity of ~40 pA on ^{44}Ca was achieved. Mass 43.5 was continuously monitored to assess potential doubly charged Sr; the contribution of Sr to the Ca isotope ratio was consistently less than 0.01‰. Instrument precision was assessed by

running in-house Ca standards, and accuracy and external precision was assessed by repeated analyses of seawater ($\delta^{44/42}$Ca = 0.96 ± 0.11‰ (n=8, chemistry=7), in keeping with previously cited long-term reproducibility (Reynard *et al.,* 2011). The uncertainties in measured isotopic analyses are given as two standard deviations of repeated analyses.

3. Results

The temporal evolution of the chemical and isotopic composition of the fluid, as well as the mass of fluid remaining in the reactor after each sample in experiments A and B are listed in Tables 1 and 2; the temporal evolution of Ca concentration and isotopic composition during these experiments are shown in Figs. 2 and 3. The $\delta^{44/42}$Ca of the original calcite grains in experiment A was -0.25±0.08 ‰. The dissolution of calcite during the first 25 hours of the experiment performed in an aqueous 0.01 mol/kg NaCl solution leads to a fluid phase Ca concentration of 0.22×10^{-3} mol/kg and a $\delta^{44/42}$Ca of 0.01±0.03‰; this latter value is 0.26‰ greater than that of the dissolving calcite. The fluid phase is calculated to be slightly supersaturated with respect to calcite at this time, which may be the result of either analytical uncertainty on the pH, alkalinity, and aqueous Ca measurements, and/or due to the presence of minor high-energy surfaces or ultra fine particles, unobserved by SEM, in the original calcite powder. The reactor fluid was then bubbled with pure CO_2, which decreased its pH to 6.2 and provoked further calcite dissolution. The fluid phase Ca concentration increased to ~4.5×10^{-3} mol/kg after ~96 hours of elapsed time then remained close to constant. The saturation state of the reactive fluid was no greater than 0.09 from this time until the end of this experiment, consistent within uncertainty of calcite equilibrium. The isotopic composition of the fluid phase, however, evolved continuously during this

239 dissolution leg of the experiment. The $\delta^{44/42}$Ca of the fluid phase was 0.34±0.06‰ 23 hours
240 after the pH change; this increased to 0.57±0.01‰ before the fluid pH was increased after
241 218 hours of elapsed time. These values are 0.45‰ and 0.72‰ greater than the initial
242 dissolving calcite. Changing the bubbling gas in the reactor to a CO_2/N_2 mixture after 218
243 hours increased the fluid pH to 7.5 leading to calcite precipitation. Calcite precipitation
244 lowered the fluid phase Ca concentration to $1.8x10^{-3}$ mol/kg; this concentration was
245 constant and within analytical uncertainly of calcite-fluid equilibrium for the final 140 hours
246 of the experiment. Despite the fact that the fluid phase was in chemical equilibrium with
247 calcite over this period, the fluid-phase Ca isotopic composition evolved substantially. The
248 fluid phase $\delta^{44/42}$Ca first increased from 0.57±0.01 to 1.15±0.04‰ after the onset of
249 precipitation, then decreased to ~0.8‰ at the end of the experiment. Mass balance
250 calculations indicate that after calcite dissolution during the dissolution leg, 18% of the Ca in
251 the system was in the fluid phase. This was lowered to 9% during the precipitation leg.

252 The evolution of the fluid phase composition of experiment B is shown in Fig. 3. The
253 $\delta^{44/42}$Ca of the original calcite grains in experiment B, which were obtained from a distinct
254 container of Merck reagent grade calcite as that of experiment A, was 0.12±0.07‰. The
255 fluid in this experiment was constantly bubbled with pure CO_2 such that the fluid pH
256 remained at a near constant 6.3. Calcite dissolved rapidly, the fluid phase attained a Ca
257 concentration of 9.5×10^{-3} mol/kg, consistent, within uncertainty, with calcite equilibrium,
258 after less than 28 hours and remained near this concentration through the end of the
259 experiment. The isotopic composition of the fluid, however, increased with time throughout
260 the experiment, increasing from 0.22±0.06‰ to ~0.6‰ after the aqueous Ca concentration
261 attained a close to constant value at near to calcite-fluid chemical equilibrium conditions.
262 These fluid Ca isotopic compositions are substantially heavier than that measured in the

solid calcite before and after the experiment. After calcite-fluid equilibrium was attained, roughly 45% of the Ca in the system was present in the fluid phase.

Photomicrographs of the calcite following experiments A and B are shown in Fig 1. In both cases only calcite is present in the post-experiment solids. Similarly post-experiment analysis of the solids recovered from these experiments by XRD revealed the presence of only calcite. The calcite recovered from experiment B shows the effect of dissolution; dissolution appears to be driven by the removal of material from the corners of calcite crystals rather than due to the formation of etch pits. This behavior is consistent with dissolution occurring at near to equilibrium conditions where there is insufficient driving force to create etch pits. Note also that as 45% of the calcite dissolved during experiment B is it possible some of the smaller grains dissolved completely. The calcite recovered from experiment A has far fewer steps than that recovered from experiment B, likely due to the precipitation of calcite onto pre-dissolved grains.

4. Discussion

4.1 Isotope release during congruent calcite dissolution and at bulk equilibrium

Results indicate that Ca isotopes fractionated during congruent calcite dissolution. Evidence that calcite dissolved congruently during the dissolution experiments include 1) the results of thermodynamic calculations demonstrating that the fluid phase was either undersaturated or in equilibrium within uncertainty with respect to calcite, and undersaturated with respect to other potentially precipitating phases during the dissolution leg of experiment A, and throughout experiment B, and 2) the SEM images after the experiments indicate the presence of only calcite in the solid phase. Moreover, the temporal

evolution of reactive fluid Ca concentrations calculated using calcite dissolution and precipitation rates reported by Chou *et al.* (1989) together with calcite solubility constants generated using PHREEQC match closely those measured in the reactors (See Figs 2a and 3a). As a result of calcite dissolution in experiment A, the measured $\delta^{44/42}$Ca of the fluid phase evolved to 0.57±0.01‰ compared to the δ^{44}Ca of -0.25±0.08‰ of the original calcite. The change in the Ca isotopic composition of the calcite due to dissolution in experiment A was not determined directly; although the Ca isotopic composition of the final solids recovered from this experiment was measured, these solids experienced both dissolution and subsequent precipitation. Nevertheless, because the experiment initially consisted of calcite and a Ca-free fluid phase, the change in the calcite bulk Ca isotope composition during this experiment can be computed from the measured isotopic composition of the fluid phase via mass conservation taking account of

$$\delta^{44/42}\mathrm{Ca}_{initial\ solid} m_{\mathrm{Ca},initial\ solid} = \delta^{44/42}\mathrm{Ca}_{solid} m_{\mathrm{Ca},solid} + \delta^{44/42}\mathrm{Ca}_{fluid} m_{\mathrm{Ca},fluid} \quad (3)$$

where $m_{\mathrm{Ca},i}$ refers to the mass of calcium in the *i*th phase, and the subscripts $initial\ solid$, $solid$, and $fluid$ designate the original solid, and the solid and fluid phase present in the reactor at the time of interest. This calculation was performed iteratively using an excel spreadsheet using the data summarized in Table 1. At each time interval, delineated by the sampling times, the Ca isotope composition of calcite was determined taking account of the mass and composition of the fluid remaining in the reactor and that removed by sampling over time. This calculation indicates that following just the 'dissolution leg' of experiment A, the bulk calcite obtains a $\delta^{44/42}$Ca of -0.42‰, a decrease of 0.17‰ during 9 days of calcite-fluid interaction at ambient temperature. The decrease between the bulk $\delta^{44/42}$Ca of the calcite before and after the 8 days of dissolution during experiment B was measured directly

and determined to be 0.19‰. The degree to which the calcite was isotopically homogeneous was not determined either before or after the experiments. It is also possible that Ca isotopes are heterogeneously distributed in the solids at the end of the experiments due to sluggish solid-state transport rates. Note that although isotopic heterogeneities in the solid phase could have accounted for the difference in isotopic compositions between the bulk original calcite and the reactive fluid during the first ~24 hours of the dissolution leg of experiment A and experiment B, the calcium isotope compositions of the reactive fluids continued to increase after this fluid attained chemical equilibrium with respect to calcite.

The exact mechanism by which isotopes fractionate during congruent calcite dissolution and at equilibrium is somewhat uncertain. Either some mechanism must allow isotopically heavy Ca to be preferentially released from the calcite structure during forward dissolution or lighter calcium needs to be returned from the fluid to the calcite during reverse precipitation. The first mechanisms seems rather unlikely, as earlier work on mineral dissolution suggest that in both carbonates and silicate minerals, lighter isotopes are preferentially released to the fluid phase at the onset of dissolution. This is because lighter isotopes generally form weaker bonds that require less energy to break (see Oelkers et al., 2015, 2018; Maher et al., 2016). Moreover, the transport of calcium, either through the fluid or solid phase would favor the transfer to the fluid of light rather than heavy Ca. The second mechanism, however, seems to be more likely as isotopic fractionation favors the incorporation of light Ca into the calcite structure during its rapid precipitation (Lemarchand *et al.,* 2004; Gussone *et al.,* 2005; Reynard *et al.,* 2011; Tang *et al.,* 2008, 2012). As such it seems likely that the observed fractionation of Ca isotopes into the fluid phase during congruent dissolution and at equilibrium stems from the two-way transfer of Ca between calcite and the fluid phase. Such a process could proceed by the conservative release of Ca

from the calcite surface coupled to fractionation during its reincorporation into the solid calcite. At bulk chemical equilibrium, this overall process would both maintain a constant fluid Ca concentration and evolve the fluid-mineral system towards isotopic equilibrium. This possibility is favored by the observation that the isotopic composition of the fluid phase evolves after the fluid has attained bulk chemical equilibrium with the dissolving calcite (see Figs 2 and 3). This possibility is also consistent with the concept of dynamic equilibrium (e.g. Aagaard and Helgeson, 1982; Oelkers *et al.,* 1994; Schott and Oelkers, 1995; Oelkers, 2001; Schott et al., 2009, 2012; Steefel et al., 2014; Lui et al. 2016). Note that a number of studies have attempted to recover bulk mineral dissolution rates at close to equilibrium conditions by measuring the temporal evolution of the isotopic composition of minerals and/or their co-existing fluids (c.f. Gruber *et al.,* 2013; Zhu et al., 2014; Subhas et al., 2015, 2017; Liu et al., 2016; Naviaux et al., 2019). It follows from the results presented in this study that such efforts need to take explicit account of the role of mineral-fluid isotope exchange during congruent dissolution and at bulk equilibrium to accurately retrieve near to equilibrium bulk dissolution rates.

The observations of isotopic equilibration during the congruent dissolution and at equilibrium in the present study differ fundamentally from the resetting of isotopic compositions of biogenic carbonates as reported by Chanda et al. (2019). This former study considered the temporal evolution of Ca isotope compositions in carbonate minerals that contained substantial Mg in its structure placed in an initially Mg-free aqueous solution. This resulted in the incongruent dissolution of the original biogenic carbonate, where the original Mg bearing carbonate was replaced by a more stable Mg-poor calcite. The observed Ca isotope composition evolution in the solids was thus driven by the thermodynamic instability of the solids placed in the reactor. In contrast, the calcite in the present study dissolved

congruently and approached a stable bulk chemical equilibrium. Isotopic evolution in the experiments performed in the present study was thus driven by the isotopic disequilibrium in the water-mineral system.

Although the net mass of total calcium transferred from the calcite to the fluid phase via calcite dissolution is readily determined from the aqueous Ca concentrations (c.f. Fig 2b), it is challenging to estimate the fraction of the Ca in the original calcite transferred to the fluid and that reincorporated into the solid during each bulk reactor dissolution experiment. A crude estimate can be made by assuming that the Ca isotopic composition of the solid at the end of the dissolution experiments consisted of a fraction, *f*, of the Ca from the original bulk calcite and a fraction 1-*f* of Ca in isotopic equilibrium with the final fluid with a fractionation factor equal to $\mathbf{\Delta}^{44/42}\mathrm{Ca}_{\text{calcite-fluid}}$. Note such estimates do not take account of changing fluid compositions during water-mineral interaction, so tend to underestimate the overall mass of calcium exchanged. Taking account these assumptions and mass balance requires that

$$\delta^{\frac{44}{42}}\mathrm{Ca}_{final\ solid} = f\delta^{44/42}\mathrm{Ca}_{initial\ solid} + (1-f)\delta^{44/42}\mathrm{Ca}_{final\ fluid} - \mathbf{\Delta}^{44/42}\mathrm{Ca}_{calcite-fluid} \quad (4)$$

The results of this calculation obtained from Eqn. (4) are shown in Fig 4 for the case of the dissolution leg of experiment A. In accord with these calculations, more than 90% of the Ca present in the original calcite powder would have equilibrated isotopically with the fluid phase during the dissolution leg of this experiment to attain the fluid phase $\delta^{44/42}$Ca observed at the end of the dissolution experiment for all $\mathbf{\Delta}^{44/42}\mathrm{Ca}_{\text{calcite-fluid}}$ < -0.9 and more than 30% for all $\mathbf{\Delta}^{44/42}\mathrm{Ca}_{\text{calcite-fluid}}$ < -1.6. The observed fluid phase $\delta^{44/42}$Ca could not be attained with any $\mathbf{\Delta}^{44/42}\mathrm{Ca}_{\text{calcite-fluid}}$ < -0.82. This comparison suggests that a majority of the

calcium present in the initial calcite grains were transferred into and out of the fluid phase during the 8 to 9 day dissolution experiments performed in this study.

4.2 Ca Isotope evolution during precipitation

The variation of reactive fluid phase $\delta^{44/42}$Ca as a function of time during the precipitation leg of experiment A is similar to that predicted by Steefel et al. (2014) for the precipitation of calcite in a closed system reactor. An initial stage of Ca isotope fractionation is observed due to the kinetically controlled preferred incorporation of light Ca into the precipitated calcite during the rapid precipitation of the mineral. This initial stage is followed by a longer stage of isotopic re-equilibration. Within the Steefel et al. (2014) formalism, this isotopic re-equilibration is a direct consequence of dynamic equilibrium; the combined effects of reverse precipitation coupled to forward dissolution, which are equal at bulk chemical equilibrium, tends to drive the mineral-fluid system towards isotopic equilibrium after the calcite has precipitated.

Further insight into the evolution of the fluid phase calcium isotopic composition during the calcite precipitation experiment can be gained with the aid of Fig. 5, which compares the evolution of reactive fluid $\delta^{44/42}$Ca as a function of *F*, the fraction of Ca precipitated from the fluid during the experiment. The curves in this figure were calculated assuming Rayleigh fractionation and equilibrium fraction (see Johnson *et al.,* 2004; Pearce *et al.,* 2012) by assuming a calcite-fluid equilibrium fractionation factor of 0.4. Rayleigh fractionation is consistent with the one-way transfer of material from the fluid phase into the solid, whereas equilibrium fractionation requires the two-way transfer of material to and from the precipitated solid. It can be seen that measured reactive fluid δ^{44}Ca is initially consistent with Rayleigh fractionation, but that $\delta^{44/42}$Ca evolves to become consistent with

equilibrium fractionation later in the experiment, while the calcite-reactive fluid system is at chemical equilibrium within analytical uncertainty. This behavior is itself consistent with kinetic theory; precipitation at far from equilibrium conditions is dominated by the transfer of material from the fluid to the solid, whereas two way transfer dominates near and at equilibrium in accord with the concept of dynamic equilibrium (e.g. Schott and Oelkers, 1995; Oelkers, 2001; Schott *et al.,* 2009; see also Pearce *et al.,* 2012).

An open question remains as the origin of the distinct behavior of calcium isotopic transfer during dissolution and during precipitation in these experiments. The Ca isotope fractionation during mineral precipitation was consistent with an equilibrium Ca fractionation factor of ~0.4, whereas that observed during calcite dissolution apparently exceeds 0.8. One possible explanation for these contrasting equilibrium fractionation factors is the distinct pH of the two experiments. The dissolution experiment presented in this study was performed at pH 6.2, whereas the precipitation experiment was performed at pH 7.5. Calcite dissolution rates are approximately 1.5 orders of magnitude faster at pH 6.2 compared to pH 7.5 (e.g. Chou et al., 1989; Cubillis et al., 2005). According to Tang *et al.* (2008) this difference in reaction rates can more than double the Ca fractionation factor between calcite and its co-existing aqueous fluid. The difference in pH of the fluid phase however may also provoke a change in the Ca isotope fractionation due a change in aqueous Ca speciation. The isotopic fractionation among aqueous species stems from the change in coordination observed between aqueous Ca^{2+} and Ca-bearing complexes (see Moynier and Fujii, 2017) and has been experimentally shown to be an important fractionation mechanism for a number of divalent cations such as Mg and Zn (Schott et al., 2016; Mavromatis et al., 2019).

An alternative explanation for different observed fractionation factors in the different experimental conditions is that the closed system experiments may not have completely attained fluid-mineral isotopic equilibrium. Such uncertainties could be overcome through the use of the three-isotope method to determine unambiguously both isotopic exchange rates at bulk mineral fluid equilibrium as well as the equilibrium isotopic fractionation factor in aqueous fluid-mineral systems (e.g. Beard *et al.*, 2010; Li *et al.,* 2011, 2014; Frierdich *et al.,* 2014; Reddy *et al.,* 2015; Zheng *et al.*, 2016; Stamm *et al.*, 2018).

4.3 Preservation of isotopic signatures in natural systems

The results reported in this study appear to contravene the commonly held assumption that calcite can preserve its isotopic signatures over geological timeframes if fluid-mineral isotopic disequilibrium exists, even if the fluid-mineral system is at bulk chemical equilibrium. This observation is not unique to either calcite or the carbonate minerals. Similar observations have been reported for the carbonates dolomite (Perez-Fernandez et al., 2017), hydromagnesite (Oelkers et al., 2018) and other hydrous Mg-carbonates (Mavromatis et al., 2012, 2015), strontianite (Mavromatis et al., 2017a), and witherite (Mavromatis et al., 2016), as well as non-carbonate minerals including goethite (Beard *et al.,* 2010; Ready *et al.,* 2015), epsonite (Li *et al.,* 2011), brucite (Li *et al.,* 2014), quartz (Lui et al., 2016), and amorphous SiO_2 (Stamm *et al.,* 2018). It follows that isotopic preservation of the original Ca signature of calcite would require either the isolation of the calcite-fluid system from external Ca input, by a process that decreases dramatically the rock permeability or the slowing of the coupled mineral dissolution/precipitation reactions. There is some indication that such processes are common in some natural systems. Turchyn and

448 DePaolo (2011) noted that much anecdotal evidence suggests that carbonate fossils are best
449 preserved in clay or organic-rich sedimentary horizons. The presence of clay minerals can
450 dramatically lower host rock permeability (e.g. Klimentos and McCann, 1990; Revel and
451 Cathels, 1999; Luijendijk and Gleeson, 2015) and thereby aid in the isolation of the fluid
452 system from external inputs. As a relatively small fraction of the Ca in most natural rocks is
453 present in the fluid phase, changes in fluid-mineral Ca isotopic fractionation due to
454 temperature changes would negligibly alter the isotopic signature of the calcite present in an
455 isolated system. Similarly, the presence of aqueous organic compounds may aid in the
456 preservation of isotopic compositions of calcite. Although they likely do not alter significantly
457 the dissolution rates of calcite (Oelkers *et al.,* 2011), the presence of aqueous organic
458 compounds can dramatically inhibit calcite precipitation (e.g. Meldrum and Hyde, 2001; de
459 Leeuw and Cooper, 2004; Lakshtnov *et al.,* 2011; Nielsen et al., 2012; Mavromatis et al.,
460 2017c). As such it appears that Ca isotopic equilibration in the presence of aqueous organic
461 compounds may be slowed by a decrease in the rate of attachment of Ca to the calcite
462 surface. Moreover the presence of aqueous Mg has also been observed to slow calcite
463 precipitation rates (e.g. Fernandez-Diaz et al., 1996; Morse et al., 2007).

464 The results presented above suggest that isotopic exchange in calcite may be rapid
465 and stems from a coupled forward dissolution/reverse precipitation process. It seems likely,
466 therefore that the preservation of isotopic signals would be favored in minerals that have
467 relatively slow dissolution rates, or those that do not precipitate at ambient temperatures.
468 For the case of preserving calcium isotopic signals, apatite dissolves ~5 orders of magnitude
469 slower at ambient conditions and seawater pH (c.f. Plummer *et al.* 1979; Chou *et al.,* 1989;
470 Valsami-Jones *et al.,* 1998; Cubillis *et al.,* 2005; Chaïrat *et al.,* 2007). It therefore seems likely
471 that apatite may be a far better guardian of original Ca isotopic signatures than calcite. For

the case of carbonate minerals, dolomite or magnesite do not appear to precipitate via abiotic processes at ambient temperatures (e.g. Saldi *et al.,* 2009, 2012; Gautier et al., 2014). As such these minerals may better preserve original C and Mg and/or Ca isotopic signatures than calcite.

5. Conclusions

The results of this study demonstrate isotopic compositions of calcite and its co-existing fluid phase can be reset rapidly by congruent dissolution, precipitation, and at equilibrium. As such the preservation of original Ca isotopic signatures in calcite may require that the calcite is isotopically isolated from its surroundings, or a not yet to be identified preservation mechanism is at play. Moreover, if the release of metals from minerals is isotopically non-conservative as seems to be the case for calcite, it may not possible to use the stable isotopic compositions of fluids to determine the source of metals, for example of environmental pollutants. Such conclusions call for further investigation of the rates and mechanisms of near to bulk equilibrium isotopic exchange to assess how best to interpret the isotopic signals recorded in minerals and natural fluids.

Acknowledgements - We are grateful to Chen Zhu, Jacques Schott, Oleg Pokrovsky, Andrea Perez-Fernandez, Nik Berninger, Franziska M. Stamm, Anna Harrison, Carl Steefel, Jenny Druhan for encouragement and insightful discussion. We would also like to thank Alain Castillo, Carol Causserand, and Thierry Aigouy for technical support. This study has been supported by the Centre National de la Recherche Scientifique (CNRS), the European Commission through Marie Cuire ITN projects MINSC (290040), METRANS (123456), and CO2-REACT (317235). Isotopic analyses and PPvS were funded by NERC fellowship NE/I020571/1.

References

Aagaard P. and Helgeson H.C. (1982) Thermodynamic and kinetic constraints on reaction-rates among minerals and aqueous solutions. 1. Theoretical considerations. *Am. J. Sci*. **282**, 237-285.

AlKhatib M. and Eisenhauer A. (2017) Calcium and strontium isotope fractionation in aqueous solutions as a function of temperature and reaction rate: I. Calcite. *Geochim. Cosmoshim. Acta* **209,** 298-319.

Beard B.L., Handler R.M., Scherer M.M., Wu L., Czaja A.D., Heimann A. and Johnson, C.M. (2010) Iron isotope fractionation between aqueous ferrous iron and goethite. *Earth Planet. Sci. Lett.* **295,** 241–250.

Blattler C.L., Jenkyns H.C., Reynard L.M. and Henderson G.M. (2011) Significant increases in global weathering during Oceanic Anoxic Events 1A and 2 indicated by calcium isotopes. *Earth Planet. Sci. Let.* **309***,* 77-88.

Brunauer S., Emmett P, H., and Teller E. (1938) Adsorption of Gases in Multimolecular Layers. *J. Am. Chem. Soc.* **60**, 309-319

Cenki-Tok B., Chabaux F., Lemarchand D., Schmidt A.D., Pierret M.C., Viville D., Bagard M.L. and Stille, P. (2009) Then impact of water-rock interaction and vegetation on calcium isotope fractionation in soil- and stream waters of a small forested catchment (the Strengbach case). *Geochim Cosmochim. Acta* **73,** 2215-2228.

Chaïrat C., Schott J., Oelkers E. H., Lartigue J.-E. and Harouiya N. (2007) Kinetics and mechanism of natural fluorapatite dissolution at 25 °C and pH from 3 to 12. *Geochim Cosmochim Acta* **71,** 5901-5912.

Chanda, P., Gorski, C.A., Oakes, R.L., and Fantle, M. S., (2019) Low temperature stable recrystallization of foraminifera tests and implications for the fidelity of geochemical proxies. *Earth Planet Sci., Let.* **506,** 428-440.

Chou L., Garrels R.M. and Wollast, R. (1989) Comparative study of the kinetics and mechanisms of dissolution of carbonate minerals. *Chem. Geol.* **78**, 269-282.

Chu N.-C., Henderson G.M., Belshaw N.S. and Hedges R.E.M. (2006) Establishing the potential of Ca isotopes as proxy for consumption of dairy products. *App. Geochem.* **21,** 1656-1667.

Cubillas P., Köhler S.J., Prieto M., Chaïrat C. and Oelkers E.H. (2005) Experimental study of the dissolution rates of calcite, aragonite, and bivalves. *Chem. Geol.* **216**, 59-77.

Curti E., Fujiwara K., Iijima K., Tits J., Cuesta C., Kitamura A., Glaus M.A. and Muller, W. (2010) Radium uptake during barite recrystalisation at 23 ±Ra°C as a function of solution composition: An experimental ^{133}Ba and ^{226}Ra tracer study. *Geochim Cosmochim. Acta* **74,** 3553-3570.

De Leeuw N.H. and Cooper T.G. (2004) A computer modeling study of the inhibiting effect of organic absorbates on calcite crystal growth. *Cryst. Growth Des.* **4,** 123-133.

DePaolo D.J. (2004) Calcium isotope variations produced by biological, radiogenic and nucleosynethetic processes. *Rev. Min. Geochem.* **55,** 255-288.

538 Druhan J.L., Steefel C.I., Williams K.H. and DePaolo D.J. (2013) Calcium isotope fractionation
539 in groundwater: Molecular scale processes influencing field-scale behavior. *Geochim*
540 *Cosmochim. Acta* **119,** 93-116.

541 Fantle M.S. (2015) Calcium isotopic evidence for rapid recrystallization of bulk marine
542 carbonates and implications for geochemical proxies. Geoc*him. Cosmochim. Acta* **148**
543 378-401.

544 Fantle M.S. and DePaolo D.J. (2007) Ca isotopes in carbonate sediment and pore fluid from
545 ODP Site 807A: the Ca^{2+}(aq)-calcite equilibrium fractionation factor and calcite
546 recrystallization rates in Peistocene sediments. *Geochim. Cosmochim. Acta* **71,** 2524-
547 2546.

548 Fantle M.S. and Higgins J. (2014) The effects of diagenesis and dolomitiation on Ca and Mg
549 isotopes in marine platform carbonates: Implications for the global cycles of Ca and Mg.
550 *Geochim. Cosmochim. Acta* **142,** 458-481.

551 Fantle M.S., Maher K.M., and DePaolo D.J. (2010) Ca isotopic approaches for quantifying
552 rates of marine burial diagenesis. *Rev. Geophys.* **48***,* RG302.

553 Fantle M.S. and Tipper E.T. (2014) Calcium isotopes in the global biogeochemical Ca cycle:
554 Implications for development of a Ca isotope proxy. *Earth. Sci. Rev.* **129,** 148-177.

555 Fairchild I.J., Smith C.L., Baker A., Fuller L., Spotl C., Mattey D. and McDermott F. (2006)
556 Modification and preservation of environmental signals in speleotherms. *Earth-Sci.*
557 *Revs.* **75,** 105-153.

558 Farkas J., Fryda J. and Holden C. (2016) Calcium isotope constraints on the marine carbon
559 cycle and $CaCO_3$ deposition during the Silurian (Ludfordian) positive delta ^{13}C excursion.
560 *Earth Planet Sci Let.* **451,** 31-40.

561 Fernandez-Diaz L., Putnis A., Prieto M., Putnis C.V. (1996) The role of magnesium in the
562 crystallization of calcite and aragonite in a porous medium. *J. Sed. Res.* **66,** 482-491.

563 Frierdich A.J., Beard B.L., Scherer M.M. and Johnson, C.M. (2014) Determination of the
564 Fe(II)aq–magnetite equilibrium iron isotope fractionation factor using the three-isotope
565 method and a multi-direction approach to equilibrium. *Earth Planet. Sci. Lett.* **391,** 77–
566 86.

567 Gautier, Q., Bénézeth, P., Mavromatis, V., Schott, J., 2014. Hydromagnesite solubility product
568 and growth kinetics in aqueous solution from 25 to 75°C. *Geochim. Cosmochim. Acta*
569 **138**, 1-20.

570 Grazis C. and Feng X.H. (2004) A stable isotope study of soil water: Evidence for mixing and
571 preferential flow paths. *Geoderma* **119,** 97-111.

572 Gruber C., Harpaz L., Zhu C., Bullen T.D. and Ganor J. (2013) A new approach for measuring
573 dissolution rates of silicate minerals by using silicon isotopes. *Geochim. Cosmochim.*
574 *Acta* **104,** 261-280.

575 Gussone N., Bohm F., Eisenhaur A., Dietzel M., Heuser A., Teichert B.M.A., Reitner J.,
576 Worheide G. and Dullo W.C. (2005) Calcium isotope fractionation in calcite and
577 aragonite. *Geochim. Cosmochim. Acta* **69**, 4485-4494.

578 Gussone N. Nehrke G. and Teichert B.M.A. (2011) Calcium isotope fractionation in ikaite and
579 vaterite. *Chem. Geol.* **285,** 194-202.

580 Harouaka K., Eisenhauer A. and Fantle M.S. (2014) Experimental investigation of Ca isotope
581 fractionation during abiotic gypsum precipitation. *Geochim. Cosmochim. Acta* **129,** 157-
582 176.

583 Heuser A., Eisenhauer A., Bohm F., Wallmann K., Gussone N., Pearson P.N., Nagler T.F. and
584 Dullo W.C. (2005) Calcium, isotope (delta Ca-44/40) variations of Neogene planktonic
585 foraminifer. *Paleoceanography* **20,** DOI: 10.1029/2004PA001048.

586 Hindshaw R.S., Bourdon B., Pogge von Strandmann P., Vigier N., and Burton K., (2013) The
587 stable calcium isotopic composition of rivers draining basaltic catchments in Iceland.
588 *Earth Planet. Sci. Let.* **374,** 173-184.

589 Hindshaw R.S., Reynolds B.C., Wiederhold J.G., Kretzschmar R., and Bourdon B. (2011)
590 Calcium isotopes in a proglacial weathering environment: Damma Glacier, Switzerland.
591 *Geochim. Cosmochim. Acta* **75**, 106-118.

592 Holmden C. and Belanger N. (2010) Ca isotope cycling in a forested catchment. *Geochim.*
593 *Cosmochim. Acta* **74,** 995-1015.

594 Jacobson A.D. and Holmden C. (2008) Delta-^{44}Ca evolution in a carbonate aquifer and its
595 bearing on the equilibrium isotope fractionation factor for calcite. *Earth. Planet. Sci. Let.*
596 **270,** 349-353.

597 Johnson C.M., Beard B.L. and Albarede F. (2004) Overview and General Concepts. *Rev. Min.*
598 *Geochem.* **55**, 1-24.

599 Jost A.B., Mundil R., He B., Brown S. T., Altiner D., Sun Y., DePaolo D.J. and Payne J.L. (2014)
600 Constraining the cause of the end-Guadalupian extinction with coupled records of
601 carbon and calcium isotopes. *Earth Planet. Sci. Let.* **396,** 201-212.

602 Kasemann, S.A. Hawkesworth C.J., Prave A.R., Fallick A.E. and Person P.N. (2005) Boron and
603 calcium isotopic composition in Neoproterozoic carbonate rocks from Namibia:
604 Evidence for extreme environmental change*. Earth Planet. Sci Let*. **231,** 73-86.

605 Kasemann S.A., Pogge von Strandmann P.A.E., Prave A. R., Fallick A.E., Elliott T. and
606 Hoffmann K-H. (2014) Continental weathering following a Crygenian glaciation:
607 Evidence from calcium and magnesium isotopes. *Earth Planet. Sci. Let.* **396,** 66-77.

608 Klimentos, T. and McCann C. (1990) Relationships among compressional wave attenuation,
609 porosity, clay content, and permeability in sandstones. *Geophys.* **55***,* 998-1014.

610 Koch P. L. (1998) Isotopic reconstruction of past continental environments. *Ann. Rev. Earth*
611 *Planet. Sci.* **26,** 573-613.

612 Lakshtnov L.Z., Bovet N. and Stipp, S.L.S. (2011) Inhibition of calcite growth by alginate.
613 *Geochim. Cosmochim. Acta* **75**, 3945-3955.

614 Lemarchand D., Wasserburg G. and Papanastassiou D. (2004) Rate-controlled calcium
615 isotope fractionation in synthetic calcite. Ge*ochim. Cosmochim. Acta* **68**, 4665-4678.

616 Leng M. J. and Marshall J. D. (2004) Palaeoclimate interpretation of stable isotope data from
617 lake sediment archives. *Quarter. Sci. Revs.* **23,** 811-831.

618 Li W., Beard B.L. and Johnson C.M. (2011) Exchange and fractionation of Mg isotopes
619 between epsomite and saturated $MgSO_4$ solution. *Geochim. Cosmochim. Acta* **75,** 1814–
620 1828.

621 Li W., Beard B.L., Li C. and Johnson, C.M. (2014) Magnesium isotope fractionation between
622 brucite [$Mg(OH)_2$] and Mg aqueous species: Implications for silicate weathering and
623 biogeochemical processes*. Earth Planet. Sci. Lett.* **394,** 82–93.

624 Li X., DePaolo D.J., Wang Y.X. and Xie X.J. (2018) Calcium isotope fractionation in a silicate
625 dominated Cenozoic aquifer system. *J. Hydology* **229,** 523-533.

626 Liu, Z., Rimstidt, J.D., Zhang, Y., Yuan, H., and Zhu, C. (2016) A stable isotope doping method
627 to test the range of applicability of detailed balance. Geochem. Perspective Let. **2,** 78-
628 86.

629 Luijendijk E. and Gleeson T. (2015) How well can we predict permeability in sedimentary
630 basins? Deriving and evaluating porosity-permeability equations for non-cemented sand
631 and clay mixtures. *Geofluids* **15**, 67-83.

632 Lyons W.B., Bullen T.D. and Welch K.A. (2017) Ca isotopic geochemistry of an Antarctic
633 aquatic system. *Geophys. Res. Let*. **44,** 882-891.

634 Maher, K., Johnson, N.C., Jackson, A., Lammers, L.N., Torchinsky, A.B., Weaver, K.L., Bird,
635 D.K., Brown, G.E., 2016. A spatially resolved surface kinetic model for forsterite
636 dissolution. *Geochim. Cosmochim. Acta* **174**, 313-334.

637 Marriott C. S., Henderson G. M., Belshaw N. S. and Tudhope A. W. (2004) Temperature
638 dependence of δ^7Li, δ^{44}Ca and Li/Ca during growth of calcium carbonate. *Earth. Planet.*
639 *Sci. Let.* **222,** 615-624.

640 Marshall J.D. (1992) Climate and oceanographic isotopic signals from the carbonate rock
641 record and their preservation. *Geol. Mag.,* **129,** 143-160.

642 Mavromatis V., Pearce C. R., Shirokova L. S., Bundeleva I. A., Pokrovsky O. S., Benezeth P. and
643 Oelkers E. H. (2012) Magnesium isotope fractionation during hydrous magnesium
644 carbonate precipitation with and without cyanobacteria. *Geochim. Cosmochim. Acta* **76**,
645 161-174.

646 Mavromatis V., Bundeleva I.A., Shirokova L.S., Millo C., Pokrovsky O.S., Benezeth P., Ader M.
647 and Oelkers E.H. (2015) The rapid resetting of carbon isotope signatures of hydrous Mg
648 carbonate in the presence of cyanobacteria. *Chem. Geo.* **404,** 41-51.

649 Mavromatis V., van Zuilen, K., Purgstaller, B., Baldermann, A., Nagler, T.F. and Dietzel, M.
650 (2016) Barium isotope fractionation during witherite ($BaCO_3$) dissolution, precipitation
651 and at equilibrium. *Geochim. Cosmochim. Acta* **190**, 72-84.

652 Mavromatis V., Harrison A. L., Eisenhauer A. and Dietzel, M. (2017a). Strontium isotope
653 fractionation during strontianite ($SrCO_3$) dissolution, precipitation and at equilibrium.
654 *Geochim. Cosmochim. Acta* **218,** 201-214.

655 Mavromatis V., Purgstaller B., Dietzel M., Buhl D., Immenhauser A. and Schott J. (2017b)
656 Impact of amorphous precursor phases on magnesium isotope signatures of Mg-calcite.
657 *Earth Planet. Sci. Lett.* **464**, 227–236.

Mavromatis, V., Gonzalez, A.G., Dietzel, M., and Schott, J. (2019) Zinc isotope fractionation during the inorganic precipitation of calcite - Towards a new pH proxy. *Geochim. Cosmochim. Acta* **244**, 99-112.

Mavromatis, V., Immenhauser, A., Buhl, D., Purgstaller, B., Baldermann, A., and Dietzel, M. (2017c) Effect of organic ligands on Mg partitioning and Mg isotope fractionation during low-temperature precipitation of calcite in the absence of growth rate effects. *Geochim. Cosmochim. Acta* **207**, 139-153.

Meldrum F.C., and Hyde S.T. (2001) Morphological influence of magnesium and organic additives on the precipitation of calcite. *J. Crys. Growth* **231**, 554-558.

Morse J.W., Arvidson R.S., Luttge A. (2007) Calcium carbonate formation and dissolution. *Chem. Rev*. **107,** 342-381.

Moynier, F., and Fujii, T. (2017) Calcium isotope fractionation between aqueous compounds relevant to low-temperature geochemistry, biology and medicine. *Sci Rep* 7.

Nagler T.S., Eisenhauer A., Muller A., Hemleben C., and Kramers J. (2000) The δ^{44}Ca - temperature calibration on fossil and cultured Globigernoides sacculifer: new tool for reconstruction of past sea surface temperatures, *Geochem. Geophys. Geosyst.* 12000GC000091.

Naviaux, J.D., Subhas, A.V., Rollins, N.E., Dong, S., Berelson. W.M. and Adkins, J.F. (2019) Temperature dependence of calcite dissolution in seawater. Geoc*him. Cosmochim. Acta* **246,** 363-384.

Neilsen J.W., Sand K.K., Pedersen C.S., Lakshtanov L.Z., Winther J.R., Willemoes M. and Stipp, S.L.S. (2013) Polysaccharide effects in calcite growth: The influence of composition and branching. *Crystal Growth Des.* **12,** 4906-4910.

Oelkers E. H. (2001) General kinetic description of multioxide silicate mineral and glass dissolution. *Geochim. Cosmochim, Acta* **65**, 3703-3719.

Oelkers E. H., Schott J. and Devidal J.-L. (1994) The effect of aluminum, pH, and chemical affinity on the rates of aluminosilicate dissolution reactions. *Geochim. Cosmochim. Acta* **58**, 2011-2024.

Oelkers E.H., Golubev S.V., Pokrovsky O.S. and Benezeth P. (2011) Do organic ligands affect calcite dissolution rates? *Geochim. Cosmochim. Acta* **75,** 1799-1813.

Oelkers, E.H., Benning, L.G., Lutz, S., Mavromatis, V., Pearce, C.R., Plümper, O., 2015. The efficient long-term inhibition of forsterite dissolution by common soil bacteria and fungi at Earth surface conditions. *Geochim. Cosmochim. Acta* **168**, 222-235.

Oelkers E.H., Berninger U.-N., Perez-Fernandez A., Chmeleff J. and Mavromatis V. (2018) The temporal evolution of magnesium isotope fractionation during hydromagnesite dissolution, precipitation, and at equilibrium. *Geochim. Cosmochim. Acta* **226,** 36-49.

Owen R.A., Day C.C., Hu C.-Y., Lui Y.H., Pointing M.D., Blaettler, C.L. and Henderson, G.M. (2016) Calcium isotopes in caves as a proxy for aridity: Modern calibration and application to the 8.2 kyr event. *Earth Planet. Sci. Let.* **442,** 129-138.

Page B.D., Bullen T.D. and Mitchell M.J. (2008) Influences of calcium availability and tree species on Ca isotope fractionation in soil and vegetation. *Biogeochem.* **88**, 1-13.

699 Parkhurst D. L. and Appelo C. A. J. (1999) User's Guide to PHREEQC (Version 2) – A Computer
700 Program for Speciation, Batch- Reaction, One-Dimensional Transport, and Inverse
701 Geochemical Calculations. U.S. Geological Survey Water-Resources Investigations Report
702 99-4259, 310pp.

703 Pearce C. R., Saldi G. D., Schott J. and Oelkers E. H. (2012) Isotopic fractionation during
704 congruent dissolution, precipitation and at equilibrium: Evidence from Mg isotopes.
705 *Geochim. Cosmochim. Acta* **92,** 170-183.

706 Perez-Fernandez A., Berninger, U.-N. Mavromatis V., Pogge Von Strandmann, P.A.E. and
707 Oelkers E.H. (2017) Ca and Mg isotope fractionation during the stoichiometric dissolution
708 of dolomite at 51 to 126 °C and 5 bars CO_2 pressure. *Chem. Geol*. **467,** 76-88.

709 Plummer L.N., Wigley T.M.L. and Parkhurst D.L. (1979) Critical review of the kinetics of
710 calcite dissolution and precipitation. in: Jeune, E.A., ed., Chemical modeling in aqueous
711 systems: American Chemical Society Symposium Series 93:537-573.

712 Pruss S.B., Blatter C.L., MacDonald F.A. and Higgins J.A. (2018) Calcium isotope evidence that
713 the earliest metazoan biomineralizers forms aragonite shells. *Geology* **46,** 736-766.

714 Reddy T.R., Frierdich A.J., Beard B.L. and Johnson, C.M. (2015) The effect of pH on stable iron
715 isotope exchange and fractionation between aqueous Fe(II) and goethite. Chem. Geol.
716 397, 118–127.

717 Revel A. and Cathels L.M. (1999) Permeability of shaly sands. *Water Resour. Res.* **35,** 651-662.

718 Reynard L.M., Day C.C. and Henderson G.M. (2011) Large fractionation of calcium isotopes
719 during cave-analogue calcium carbonate growth. *Geochim. Cosmochim. Acta* **75,** 3726-
720 3740.

721 Reynard L.M., Henderson G.M. and Hedges, R.E.M. (2010) Calcium isotope ratios in animal
722 and human bone. Large fractionation of calcium isotopes during cave-analogue calcium
723 carbonate growth. *Geochim. Cosmochim. Acta* **74,** 3735-3750.

724 Ryu J.S., Jacobsen A.D., Holmden C., Lundstrom, C. and Zhang, Z.F. (2011) The major ion,
725 $\delta^{44/40}$Ca, $\delta^{44/42}$Ca and $\delta^{26/24}$Mg geochemistry of grantie weathering at pH=1 and T=25 C:
726 Power law processes and the relative reactivity of minerals. *Geochim. Cosmochim. Acta*
727 **75,** 6004-6026.

728 Saldi G.D., Jordan G., Schott, J. and Oelkers E.H. (2009) Magnesite growth rates as a function
729 of temperature and saturation state. *Geochim. Cosmochim. Acta.* **73**, 5646-5657.

730 Saldi G.D., Schott J., Pokrovsky O.S., Gautier Q. and Oelkers E.H. (2012) An experimental
731 study of magnesite precipitation rates at neutral to alkaline conditions and 100 to 200 °C
732 as a function of pH, aqueous solution composition and chemical affinity *Geochim.*
733 *Cosmochim. Acta*, **83,** 93-109.

734 Sawaki Y., Tahata M., Ohno T., Komiya T., Hirata T., Maruyama S., Han, J. and Shu D. (2014)
735 The anomalous Ca cycle in the Ediacaran ocean: Evidence from Ca isotopes preserved in
736 the Three Gorges area, South China. *Gondwana Res.* **25,** 1070-1089.

737 Shirokova L.S., Mavromatis V., Bundeleva I.A., Pokrovsky O.S., Benezeth P., Gerard E., Pearce
738 C.R. and Oelkers E.H. (2013) Using Mg isotopes to trace cyanobacterially mediated
739 magnesium carbonate precipitation in alkaline lakes. *Aquat. Geochem.* **19,** 1-24.

740 Schmitt A.D., Bracke G., Stille P. and Kierel B. (2001) The calcium isotope composition of
741 modern seawater determined by thermal ionisation mass spectrometry. *Geostandards*
742 *Newsletter* **25**, 1-9.

743 Schott J. and Oelkers E. H. (1995) Dissolution and crystallization rates of silicate minerals as a
744 function of chemical affinity. *Pure App. Chem.* **67,** 903-910.

745 Schott J., Pokrovsky O. S. and Oelkers E. H. (2009) The link between mineral
746 dissolution/precipitation kinetics and solution chemistry. *Rev. Min. Geochem.* **70**, 207-
747 258.

748 Schott J., Pokrovsky O. S. Benezeth P., Goderris Y. and Oelkers E. H. (2012) Can accurate rate
749 laws be created to describe chemical weathering? *Comptes Rendus Geosci.* **344,** 568-
750 585.

751 Schott, J., Mavromatis, V., Fujii, T., Pearce, C.R., Oelkers, E.H., 2016. The control of carbonate
752 mineral Mg isotope composition by aqueous speciation: Theoretical and experimental
753 modeling. *Chem. Geol.* **445**, 120-134.

754 Silva-Tamayo J.C., Lau K.V., Jost A.B., Payne J.L., Wignall P.B., Newton R.J., Eisenhauer A.,
755 DePaolo D.J., Brown S., Maher K., Lehrmann D.J., Altiner D., Yu M.Y., Richoz S. and
756 Paytan A. (2018) Global perturbation of the marine calcium cycle during the Permian-
757 Triassic transition. *Geol. Soc. Am. Bull.* **130,** 1323-1338.

758 Stamm F.M., Zambardi T., Chmeleff J., Schott J., von Blanckenburg F. and Oelkers E.H. (2018)
759 The experimental determination of equilibrium Si isotope fractionation factors among
760 $H_4SiO_4°$, $H_3SiO_4^-$ and amorphous silica (SiO_2·0.32 H_2O) at 25 and 75°C using the three
761 isotope method. *Geochim. Cosmochim. Acta* submitted.

762 Steefel C.I., Druham J.L. and Maher, K. (2014) Modelled coupled chemical and isotopic
763 equilibration rates. *Proced. Earth Planet. Sci*. **10,** 208-217.

764 Subhas, A.V., Rollins, N.E., Berelson, W.M., Dong, S., Erez, J. and Adkins, J.F. (2015) A novel
765 determination of calcite dissolution kinetics in seawater. *Geochim. Cosmochim. Acta*
766 **170,** 52-68.

767 Subhas, A.V., Adkins, J.F., Rollins, N.E., Naviaux, J., Erez, J., and Berelson, W.M. (2017)
768 Catalyis and chemical mechanism of calcite dissolution in seawater. *Proc. Nat. Acad. Sci.*
769 **114,** 8175-8180.

770 Tang J., Dietzel M., Böhm F., Köhler S.J. and Eisenhauer A. (2008) Sr^{2+}/Ca^{2+} and $^{44}Ca/^{40}Ca$
771 fractionation during inorganic calcite formation: II. Ca isotopes. *Geochim. Cosmochim.*
772 *Acta* **72**, 3733-3745.

773 Tang J., Niedermayr A., Köhler S.J., Bohm F., Kisakurek B., Eisenhauer A. and Dietzel M.
774 (2012) Sr^{2+}/Ca^{2+} and $^{44}Ca/^{40}Ca$ fractionation during inorganic calcite formation: III.
775 Impact of salinity.ionic strength. *Geochim Cosmochim. Acta* **77,** 432-443.

776 Teichert B.M.A., Gussone N. and Torres, M.E. (2009) Controls on calcium isotope
777 fractionation in sedimentary porewaters. *Earth Planet. Sci. Let.* **279,** 373-382.

778 Tipper E.T., Galy A. and Bickle M.J. (2006) Riverine evidence for a fractionated reservoir of Ca
779 and Mg on the continents: Implications for the oceanic Ca cycle. *Earth Planet. Sci. Let.*
780 **247,** 267-279.

781 Tipper E.T., Galy A. and Bickle M.J. (2008) Calcium and magnesium isotope systematics in
782 rivers draining the Himalaya-Tibetan plateau region: Lithogical or fractionation control?
783 *Geochim Cosmochim Acta* **72,** 1057-1075.

784 Turchyn A.V. and DePaolo D.J. (2011) Calcium isotope evidence for suppression of carbonate
785 dissolution in carbonate-bearing organic-rich sediments. *Geochim. Cosmochim. Acta* **75,**
786 7081-7098.

787 Valsami-Jones E., Ragnarsdottir K.V., Putnis A., Bosbach D., Kemp A.J. and Cressey, G., (1998)
788 The dissolution of apatite in the presence of aqueous metal cations at pH 2-7. *Chem.*
789 *Geo*. **151**, 215-233.

790 Van't Hoff, M.J.H. (1884) Etudes de dynamique chimique. *Recueil Travaux Chimiques Pas-Bas*
791 **3**, 333-336.

792 Voigt M., Marieni C., Clark D.E., Gislason, S.R. and Oelkers E.H. (2018) Evaluation and
793 refinement of thermodynamic databases for mineral carbonation. Energy Procedia **146**,
794 81-91.

795 Wang W.Z., Qin T., Zhou C., Huang S.C. Wu Z.Q. and Huang F. (2017) Concentration effect on
796 equilibrium fractionation of Mg-Ca isotopes in carbonate minerals. Insights from first
797 principle calculations. *Geochim. Cosmochim. Acta* **208,** 185-197.

798 Wiederhold J.G. (2015) Metal isotope signatures as tracers in environmental geochemistry.
799 *Envir. Sci. Tech.* **49,** 2606-2624.

800 Yan H., Schmitt A.D., Liu Z.H. Gangloff S., Sun H.L., Chen J.B. and Chabaux F. (2016) Calcium
801 isotopic fractionation during travertine deposition under different conditions: Examples
802 from Baishuitai (Yunan, SW China). C*hem. Geol.* **426,** 60-70.

803 Zheng X.-Y., Beard B.L., Reddy T.R., Roden E.E. and Johnson C.M. (2016) Abiologic silicon
804 isotope fractionation between aqueous Si and Fe(III)–Si gel in simulated Archean
805 seawater: Implications for Si isotope records in Precambrian sedimentary rocks.
806 G*eochim. Cosmochim. Acta* **187,** 102–122.

807 Zhu C., Liu Z.Y., Schaefer A., Wang C., Zhang G.R., Gruber C., Ganor J. and Gerog R.B. (2014)
808 Silicon isotopes as a new method of measuring silicate mineral reaction rates at ambient
809 temperature. *Proc. Earth Planet. Sci.* **10,** 189-193.

810 Zhu P. and Macdougall J.D. (1998) Calcium isotopes in the marine environment and the
811 oceanic calcium cycle. *Geochim.Cosmochim. Acta* **62,** 1691-1698.

812

813 **Figure Captions**

814 Figure 1. SEM images of the calcite powder used in the experiments a) the initial calcite prior
815 to experiment A, b) the calcite grains recovered after the experiment A, and c) calcite
816 grains recovered after experiment B.

817

Figure 2: Temporal chemical and isotopic evolution of the fluid phase during experiment A: a) Measured fluid phase Ca concentration, the error bars in this figure correspond to an estimated 4% uncertainty in these analyses; b) fraction of the total Ca preset in the system within calcite, the error bars in this plot represent an estimated 2% uncertainty in these values; c) fluid Ca isotopic composition; the error bars in c are taken as two standard deviations of repeated analyses. Note that the pH of the fluid phase was changed after 25 and after 125 hours, by changing the identity of the gas bubbling through the reactor. The timing of these pH changes is indicated by the vertical lines. The thin dashed curves in a were calculated using calcite dissolution/precipitation rate equations of Chou et al. (1989) whereas those in b and c are for the aid of the reader. The thick dashed line in c corresponds to the Ca isotopic composition of the original dissolving solid its associated 2 standard deviation uncertainty – see text and Table1.

Figure 3: Temporal chemical and isotopic evolution of the fluid phase during experiment B: a) Measured fluid phase Ca concentration, the estimated 4% uncertainty in these analyses is within the size of their symbol; b) fluid Ca isotopic composition; the error bars in b are taken as two standard deviations of repeated analyses. The dashed curve in a were calculated using calcite dissolution/precipitation rate equations of Chou et al. (1989) whereas that in b is for the aid of the reader. The thick grey line in c corresponds to the Ca isotopic composition of the original dissolving solid and its associated 2 standard deviation uncertainty – see text and Table1.

Figure 4. Calculated fraction of calcite present in the inital calcite (*f*) required to pass through the fluid phase to obtain the observed fluid phase Ca isotopic composition at the end of the dissolution leg of Experiment A, as a function of the equilibrium calcite-fluid Ca fractionation factor.

Figure 5: The Ca isotopic composition of the fluid phase provoked by calcite precipitation during the final 240 hours of experiment A plotted as a function of the fraction of the reactive fluid Ca incorporated into the solid. The solid curve represents the fluid composition of this fluid calculated using a Rayleigh distillation model whereas the linear curve corresponds to the fluid composition calculated with an equilibrium fractionation model. In each case the solid curves were calculated by adopting the calcium-fluid fractionation factor, $\Delta^{44/42}Ca_{fluid\text{-}solid} = -0.4$.

Table 1. Measured chemical and isotopic compostion of the fluid and solid phases during experiment A. Note that the pH of the fluid phase was changed after 25 and 218 hours of elapsed time by changing the composition of the gas bubbled through the reactor – see text.

Sample	Elapsed time (hours)	Reactive fluid mass (g)[a]	*pH*	c_{Ca} (mol/kg x10^3)	Alkalinity (eq/kg x10^3)	Percent aqueous Ca[b]	$\delta^{44/42}Ca$[c]	Saturation index[d]
A-1	25	948.2	8.39	0.22	5	0.9	0.01±0.03	0.24
A-2	48	933.3	6.23	3.85	29	15.6	0.28±0.11	-0.02
A-3	73	918.3	6.23	4.99	33	20.1	0.34±0.06	0.10
A-4	96	902.4	6.19	4.14	32	16.8	0.36±0.07	-0.02
A-5	145	886.6	6.19	4.21	32	17.0	0.55±0.04	-0.02
A-6	170	870.7	6.20	4.80	33	19.3	0.27±0.04	0.05
A-7	196	854.4	6.18	4.99	36	20.0	0.51±0.12	0.07
A-8	218	837.6	6.18	4.81	35	19.3	0.57±0.01	0.05
A-9	242	810.0	7.43	1.65	3.8	8.0	0.72±0.07	0.08
A-10	265	780.7	7.49	1.75	2.7	8.4	1.06±0.06	0.02
A-11	289	751.6	7.56	1.75	2.7	8.4	1.15±0.04	0.09
A-12	337	722.4	7.46	1.94	2.8	9.0	0.75±0.09	0.05
A-13	363	692.4	7.48	1.81	2.8	8.6	0.77±0.01	0.04
A-14	385	660.9	7.49	1.87	2.4	8.7	0.92±0.04	0.00
Initial Calcite							-0.25±0.08	
Final Calcite							-0.41±0.01	

a) Reactive fluid remaining in the reactor after the fluid sample was collected as determined by weighing the fluid samples. b) Percent of calcium in the batch reactor present in the aqueous phase as calculated from mass balance constraints. c) All $\delta^{44/42}Ca$ listed in this table were measured; listed +/- uncertainties refer to two standard deviations of repeated analyses. d) Saturation index of the sampled aqueous fluid with respect to calcite calculated using the PHREEQC computer code together with its minteq.v4 database. It is estimated that the uncertainty in calculated saturation indexes are approximately ±0.1.

Table 2. The measured chemical and isotopic compostion of the fluid and solid phases during experiment B.

Sample	Elapsed time (hours)	Reactive fluid mass (g)[a]	*pH*	c_{Ca} (mol/kg x10^3)	Alkalinity (eq/kg x10^3)	Percent Aqueous Ca[b]	$\delta^{44/42}Ca$[c]	Saturation index[d]
B-1	3	984.7	6.39	8.77	8.32	43.2	0.15±0.08	-0.01
B-2	5.5	965.7	6.21	9.31	11.49	45.9	0.22±0.06	-0.05
B-3	28	947.6	6.28	9.27	11.13	45.7	0.45±0.05	0.01
B-4	45	927.5	6.23	9.40	11.26	46.3	0.42±0.02	-0.03
B-5	70	909.3	6.25	9.42	11.24	46.4	0.50±0.04	-0.01
B-6	101	891.4	6.23	9.44	10.74	46.5	0.52±0.10	-0.03
B-7	121	875.7	6.22	9.46	11.02	46.6	0.64±0.10	-0.05
B-8	149	858.0	6.25	9.64	11.04	47.3	0.59±0.04	-0.01
B-9	172	838.5	6.25	9.66	12.03	47.4	0.52±0.03	0.02
B-10	193	814.2	6.26	9.09	10.64	45.1	0.64±0.04	-0.04
Initial Calcite							0.12±0.07	
Final Calcite							-0.07±0.02	

a) Reactive fluid remaining in the reactor after the fluid sample was collected as determined by weighing the fluid samples. b) Percent of calcium in the batch reactor present in the aqueous phase as calculated from mass balance constraints. c) All $\delta^{44/42}Ca$ listed in this table were measured; listed +/- uncertainties refer to two standard deviations of repeated analyses. d) Saturation index of the sampled aqueous fluid with respect to calcite calculated using the PHREEQC computer code together with its minteq.v4 database. It is estimated that the uncertainty in calculated saturation indexes are approximately ±0.1.

887

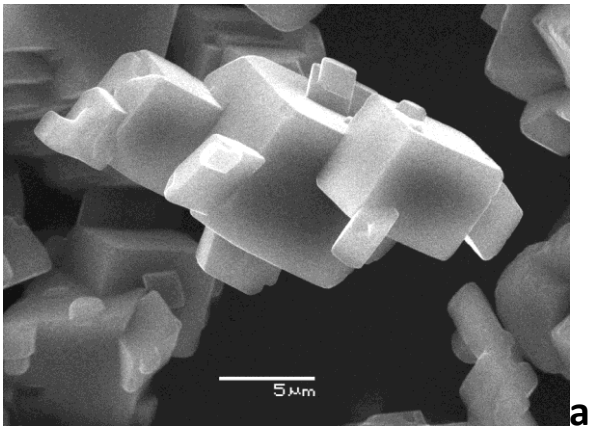

a.

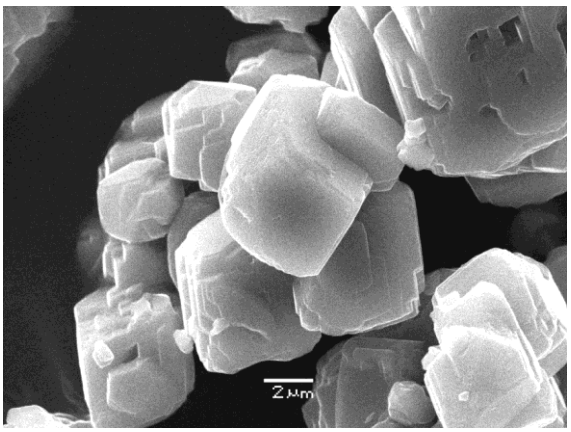

b.

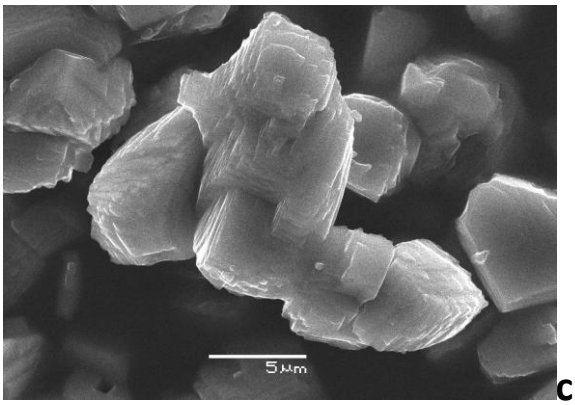

c.

888

889

890

891 **Figure 1.**

892

893

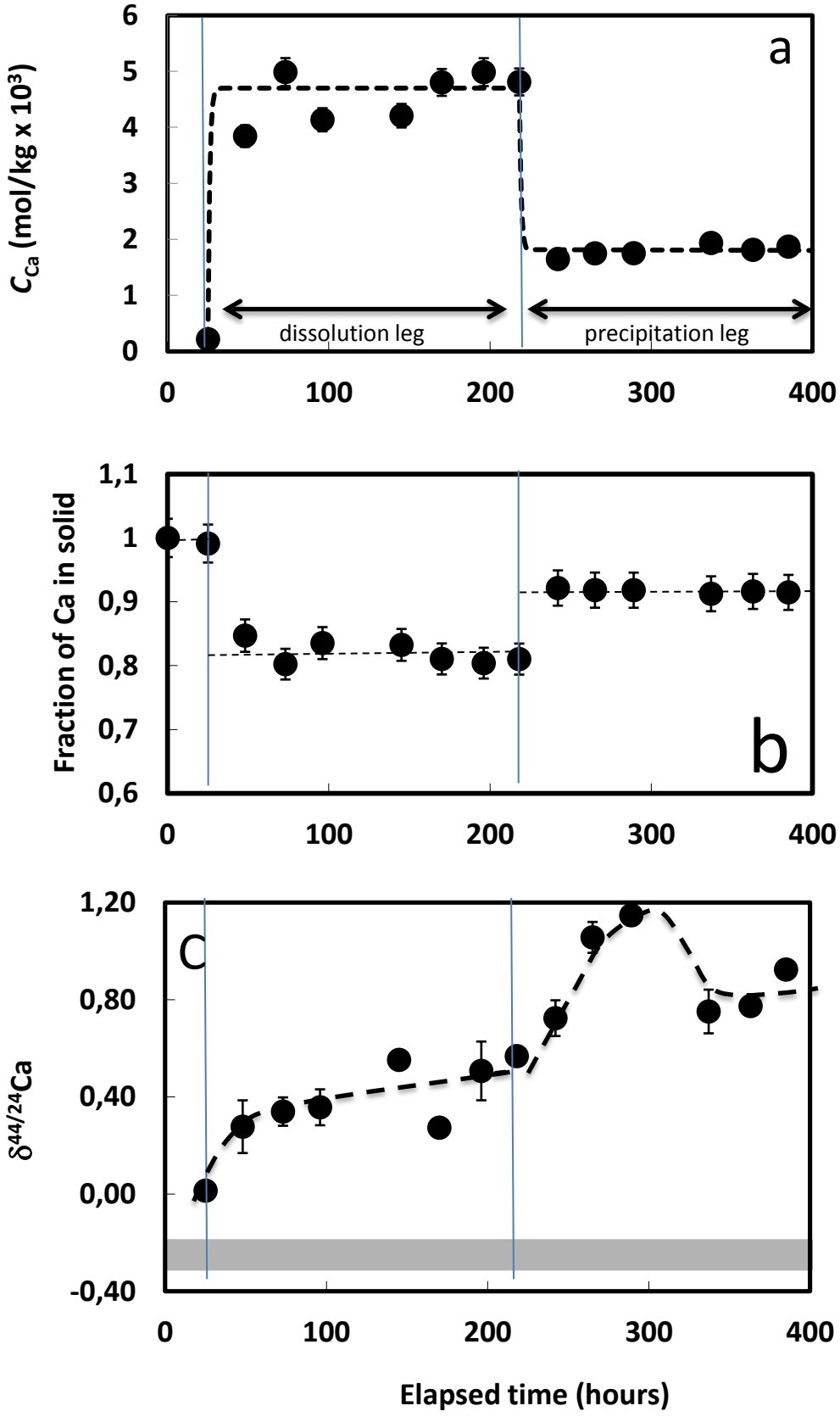
a
C_{Ca} (mol/kg x 10^3)
dissolution leg
precipitation leg
b
Fraction of Ca in solid
c
$\delta^{44/24}$Ca
Elapsed time (hours)

FIGURE 2:

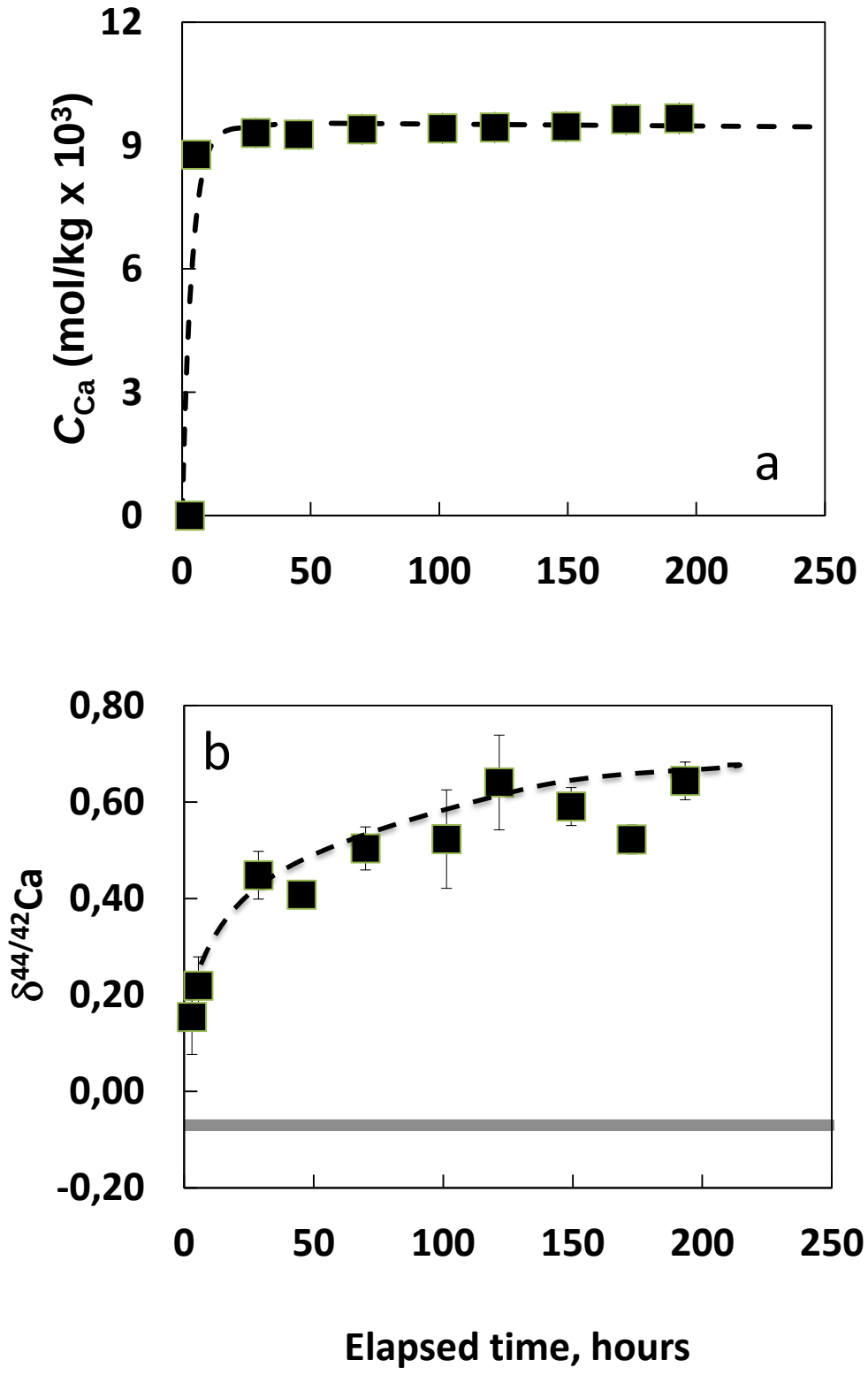

899

900
901

902 **Figure 3.**

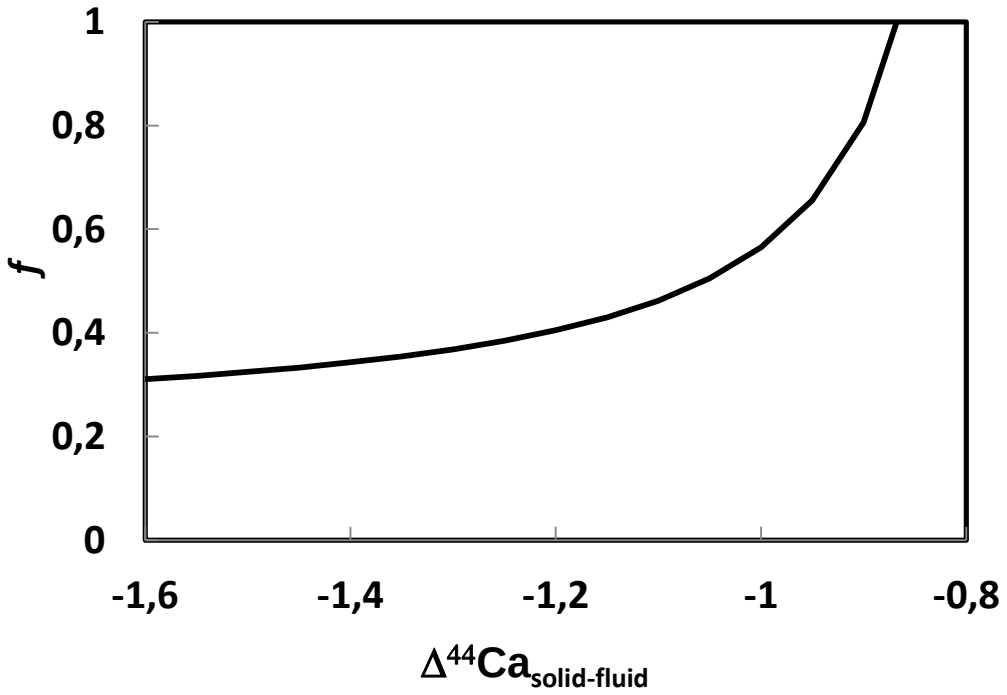

903
904

905 **Figure 4.**

906

907

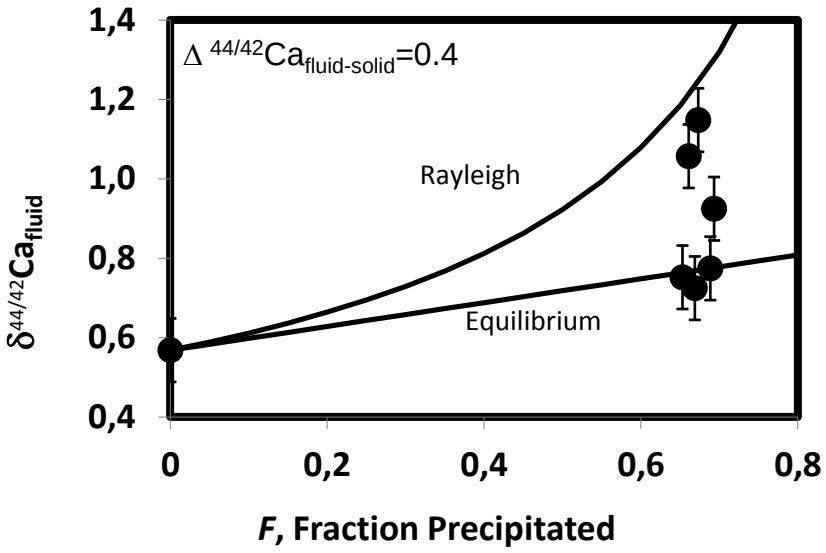

908

909 **Figure 5**

910